IEEE Access
Multidisciplinary ⋮ Rapid Review ⋮ Open Access Journal

Received January 20, 2022, accepted February 3, 2022, date of publication February 9, 2022, date of current version February 22, 2022.

Digital Object Identifier 10.1109/ACCESS.2022.3150348

Bandstop Filter Decoupling Technique for Miniaturized Reconfigurable MIMO Antenna

HASHINUR ISLAM[1], (Graduate Student Member, IEEE), SAUMYA DAS[2], TANWEER ALI[3], (Senior Member, IEEE), TANUSHREE BOSE[1], SUMANA KUMARI[4], OM PRAKASH[5], AND PRADEEP KUMAR[6]

[1]Department of Electronics and Communication Engineering, Sikkim Manipal Institute of Technology, Sikkim Manipal University, Gangtok, Sikkim 737136, India
[2]Department of Information Technology, Sikkim Manipal Institute of Technology, Sikkim Manipal University, Gangtok, Sikkim 737136, India
[3]Department of Electronics and Communication, Manipal Institute of Technology, Manipal Academy of Higher Education, Manipal 576104, India
[4]Department of Electronics Engineering, University Polytechnic, Birla Institute of Technology, Mesra, Ranchi, Jharkhand 835215, India
[5]ECE Department, Sri Venkateswara College of Engineering and Technology, Chittoor, Andhra Pradesh 517127, India
[6]Discipline of Electrical, Electronic and Computer Engineering, University of KwaZulu-Natal, Durban 4041, South Africa

Corresponding authors: Tanweer Ali (tanweer.ali@manipal.edu) and Pradeep Kumar (pkumar_123@yahoo.com)

This work was supported by the TMA Pai Research Grant, Sikkim Manipal University, Sikkim, India, under Grant/Award 118/SMU/REG/UOO/104/2019.

ABSTRACT In this work, a switchable bandstop filter is used as a decoupling structure for developing a miniaturized reconfigurable multiple input multiple output (MIMO) antenna. Initially, a dual band ((2.43-2.60 GHz and 3.51-3.79 GHz)) single monopole antenna structure is developed on FR4 substrate. Then the single monopole antenna and its replica are accommodated in a small space with an edge to edge separation distance of 11 mm to form a 2 port MIMO antenna. Now, a switchable bandstop filter is used as a decoupling network between two closely spaced monopole antenna elements to prevent mutual coupling and reconfigure the antenna characteristics. The dual pole switchable bandstop filter is configured in such a way that one of its poles lies at 2.5 GHz in one state (Mode 1) and at 3.68 GHz in another state (Mode 2) under the switching action of two PIN diodes. Controlling the ON/OFF states of the PIN diodes in the bandstop filter, high isolation is achieved alternately in lower (2.43-2.60 GHz) and upper (3.51-3.79 GHz) frequency bands of the MIMO antenna. Also, stub network is used to improve impedance matching in the upper frequency band. The proposed isolation technique helps the antenna to yield high isolation (>30 dB), fair gain (>2.97 dBi), reasonable radiation efficiency (>86.8 %), low envelope correlation coefficient (<0.16), high diversity gain (DG > 9.88 dB), low Mean effective gain ratio (MEG 1/MEG 2 < 0.05 dB) and low channel capacity loss (CCL < 0.06 bits/s/Hz) for both the operating frequency bands. The overall dimension of the antenna is restricted to 44mm × 22mm ($0.36\lambda_o \times 0.18\lambda_o$) for its easy integration in compact wireless devices. This type of reconfigurable MIMO antenna is best suited for cognitive radio communication, which promotes efficient spectrum utilization.

INDEX TERMS Bandstop filter, MIMO, reconfigurable MIMO antenna.

I. INTRODUCTION

Because of the introduction of various multimedia services, todays modern wireless communication systems can accommodate higher data rates than previous systems. Multi-element antennas, such as multiple-input multiple-output (MIMO) antenna systems, are required for these multimedia services, as they are one of the most effective strategies for enhancing channel capacity and reliability [1]. In addition to the high data rate, modern communication systems also require the ability to accommodate multiple communication standards integrated with a single antenna compact device. So, reconfigurable MIMO systems which can support multi-band communications with high data rates are in the prime focus of wireless communication research [2]. Reconfigurable MIMO systems require reconfigurable MIMO antennas for transmitting and receiving electromagnetic waves of different frequency bands. However, integrating reconfigurable MIMO antennas into a small and compact wireless device while maintaining good isolation between multiple

The associate editor coordinating the review of this manuscript and approving it for publication was Tutku Karacolak.

elements is difficult [3]. So, reconfigurable compact MIMO antennas need to address both reconfiguration and isolation challenges while restricting the antenna dimension.

The electrical length of the radiator is reorganized by frequency reconfiguration, which necessitates the use of switching circuitry to reconfigure the operating frequency bands [4]–[6]. The switching circuitry in an antenna can be realized by using various techniques, such as radio-frequency micro-electro-mechanical systems (RF MEMS) [7], Varactor diodes [8], and positive-intrinsic negative (PIN) diodes [9], etc. Although there are numerous methods for reconfiguring antenna operation, PIN-based reconfiguration has received the most attention from researchers due to its shorter response delay and compact implementation. However, integrating a PIN diode into a MIMO antenna increases the overall volume of the antenna. As a result, how to implement a compact frequency-reconfigurable MIMO antenna in a slim wireless device is an important issue.

In addition to switching action, a reconfigurable MIMO antenna has to address the isolation problem that arises due to strong mutual coupling between antenna elements [10]. Some isolation techniques such as decoupling networks [11], parasitic elements [12], defected ground plane structures [13], antenna placement and orientation [14], neutralization lines [15], metamaterial [16] metasurface [17], [18], and electromagnetic bandgap [19]–[21] are widely used to reduce the mutual coupling between antenna elements as well as antenna element and ground plane.

Reconfigurable MIMO antennas have been reported in a few peer reviewed research articles. These antennas have addressed reconfiguration as well as isolation precisely exploring various techniques. In the paper [22], PIN diode based reconfigurable technique has been implemented to design UWB/WiMAX MIMO antenna of frequency bands 1.3-12 GHz and 2.32-3.8 GHz. Defected rectangular stub line structure on the ground plane has been created for achieving isolation. But the isolation has been limited to 25-30 dB almost in the entire frequency bands. The two port MIMO antenna measures 14mm × 30mm in total dimension.

PIN diodes have also been used to bring frequency reconfiguration for a two port MIMO antenna presented in [23]. Depending on the on/off state of the PIN diode, the resonant frequency is altered between the WLAN band (2400-2483 and 5150-5350 MHz) and the m-WiMAX band (3400-3600 MHz). An isolation improvement structure on the ground plane brings the isolation at desired band maximum of 25 dB. The complete antenna has a dimension of 80mm × 40mm.

In another work, a two port compact frequency reconfigurable multiband LTE MIMO Antenna for Laptop Applications has been developed using PIN diode reconfigurability option [24]. In conjunction with the proximity-coupled feed structure, it consists of two planar Inverted-F antenna (PIFA) elements connected by a T-shaped dc line and two PIN diodes (D1 and D2). At State 1 (D1 and D2: ON state), the proposed MIMO antenna covers the LTE 17/13 bands (704-787 MHz) and the LTE 20/7 bands (791-862 MHz, 2500-2690 MHz) at State 2 (D1 and D2: OFF state). Maximum isolation of amount 35 dB has been achieved with a special orientation of MIMO antennas inside the Laptop. The antenna has an overall dimension of 5mm × 125mm.

So, the researchers have a sincere desire to improve isolation in reconfigurable MIMO antennas while minimizing dimensions. However, it is extremely rare to find a compact reconfigurable MIMO antenna with isolation greater than 35 dB. Recently, split ring resonator (SRR) based filtering technique gained popularity for achieving high isolation in compact MIMO structure [25]. This technique uses a unit cell SRR as a decoupling network and is able to increase isolation as high as 43 dB in a low profile MIMO antenna [26].

This work combines bandstop filter based isolation and PIN diode-based reconfiguration to achieve isolation greater than 35 dB and frequency reconfigurability of a MIMO antenna. A switchable bandstop filter has been considered as a decoupling network to achieve high isolation for a two port MIMO antenna. The final dimension of proposed antenna is reduced to 44mm × 22mm ($0.36\lambda_o \times 0.18\lambda_o$) for achieving a compact low profile structure. The PIN diode switching action of the filter enables the MIMO antenna to resonate at 3.68 GHz and 2.5 GHz under Mode 1 and Mode 2 operations respectively. Isolation achieved at 3.68 GHz and 2.5 GHz is 42.77 dB and 37.49 dB respectively. The performance of two port MIMO antenna at two different frequency bands are observed in terms of resonance, isolation, realized gain, radiation efficiency, radiation pattern, envelope correlation coefficient (ECC), diversity gain (DG), mean effective gain (MEG), total active reflection coefficient (TARC), and channel capacity loss (CCL). Simulation results are validated with the measured results. Comparative analysis reveals that the proposed bandstop filter reconfiguration technique-based MIMO antenna achieves greater isolation and deeper resonance than previously described antennas of comparable dimension.

II. GRADUAL PROCEDURE OF RECONFIGURABLE MIMO ANTENNA DEVELOPMENT

The reconfigurable MIMO antenna is created in four steps: Single antenna creation, Two port antenna development, Reconfigurable decoupling network development, and Reconfigurable MIMO antenna development. Gradual progress in each phase has been detailed below.

A. SINGLE ANTENNA CREATION

The development phase starts with designing a single antenna on FR4 substrate ($\varepsilon_r = 4.4$, loss tangent $\tan\delta = 0.02$) of thickness 1.6 mm as presented in Fig 1. An 'a' shaped antenna structure is created with a partial ground plane for achieving the resonance at desired LTE frequency bands. The 'a' shape structure can support two different current paths to bring dual band resonance for the single monopole antenna. The microstrip feed line is shifted from the middle of 'a' shaped structure is to achieve desired current path for accommodating centre frequencies 2.7 GHz and 3.65 GHz with the monopole antenna structure. The partial ground plane helps to increase the impedance matching for the monopole antenna. Simulation is carried out on the HFSS platform to optimize the dimensions of design parameters of single antenna. The design parameters are set as follows: $W = 22$, $W_2 = 11$, $W_3 = 9.5$, $W_4 = 10.5$, $W_5 = 7.5$, $W_6 = 1.5$, $L_1 = 22$, $L_2 = 10$, $L_3 = 3$, $L_4 = 6$, $L_5 = 10$, and $L_6 = 9$ (unit: mm). It is evident from the reflection coefficient (Fig 2) that the single antenna structure resonates at dual bands of centre frequency 2.7 GHz and 3.65 GHz with this configuration. It is developed on a substrate of dimension 22 mm × 22 mm. The current distribution displayed in Fig 3a and Fig 3b confirms the λ/4 current path length of 28 mm and 21 mm for 2.7 GHz and 3.65 GHz respectively.

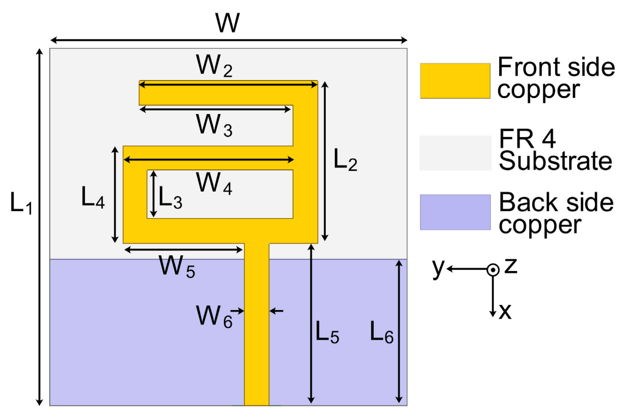

FIGURE 1. Proposed single antenna.

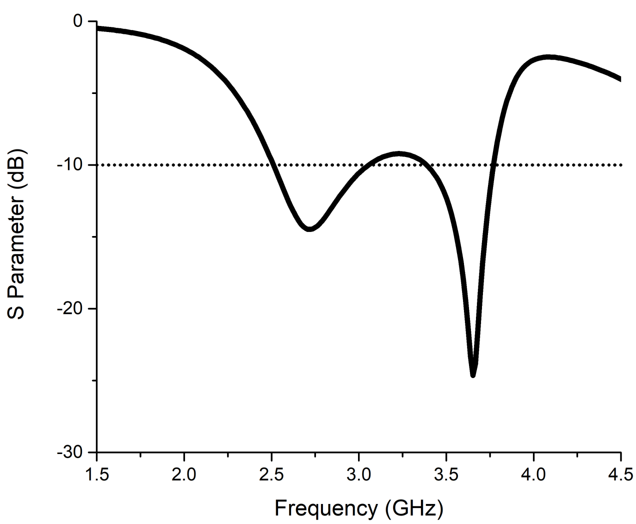

FIGURE 2. Reflection coefficient of single antenna.

B. TWO PORT ANTENNA DEVELOPMENT

The two port antenna development phase starts by including two single antenna elements on substrate dimension

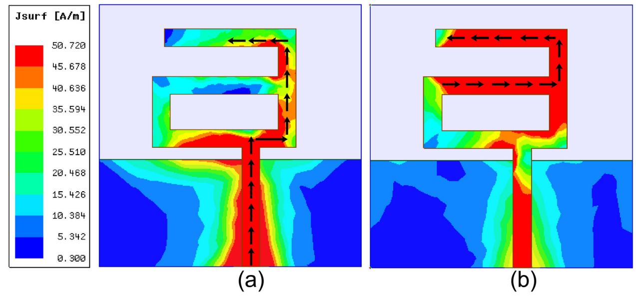

FIGURE 3. Current distribution of the proposed single antenna element at (a) 2.7 GHz and (b) 3.65 GHz.

44mm × 22mm ($W_1 \times L_1$) as shown in Fig 4. The spacing (W_8) between two antenna elements is kept as 18.5 mm. It resonates at dual bands of centre frequency 2.5 GHz and 3.68 GHz but with poor isolation, as shown in Fig 5. Although, it has been designed with a compact dimension, but unable to showcase the best performance due to high mutual coupling between antenna elements and the ground plane. The surface current distribution at 2.5 GHz and 3.68 GHz, as shown in Fig 6 and Fig 7, confirms the strong mutual coupling on the antenna element staying alongside as well as the ground plane when port 1 is activated and port 2 is terminated with a 50 Ω matched load.

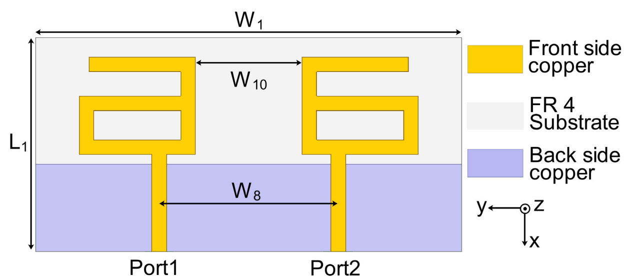

FIGURE 4. Proposed two elements antenna structure.

C. RECONFIGURABLE DECOUPLING NETWORK DEVELOPMENT

In this phase of development, efforts are made to develop a reconfigurable decoupling network. For this purpose, a dual pole reconfigurable bandstop filter exploring PIN diode integrated structure is developed, shown in Fig 8. The dual pole reconfigurable bandstop filter is configured in such a way that one of its poles lies at 3.68 GHz under the 'ON' state of PIN diodes (Mode 1). The same dual pole structure brings one of its poles at 2.5 GHz under 'OFF' state of PIN diodes (Mode 2). For the switching operation of the reconfigurable filter, SMP 1320-079 LF PIN diodes are considered. The PIN diodes are shown in Fig 9 as a series RL circuit for ON condition and a combination of parallel series RLC circuits for OFF condition. The biasing of PIN diodes is done with a 9-volt supply. The ON state resistance and inductance of these PIN diodes are Rs = 0.75 Ω and L = 0.7 nH, respectively.

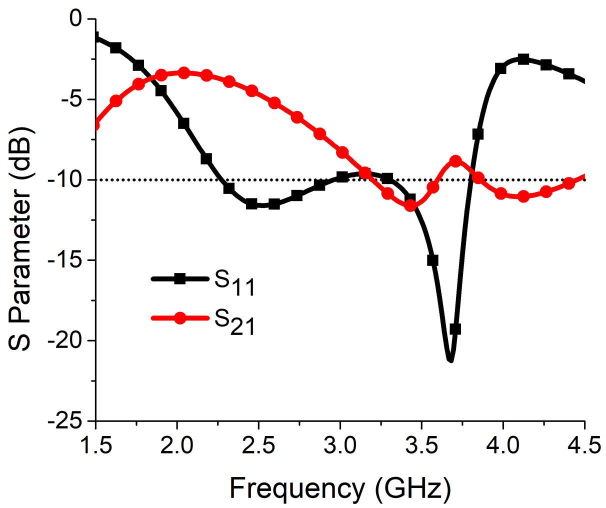

FIGURE 5. S-parameters of two element antenna.

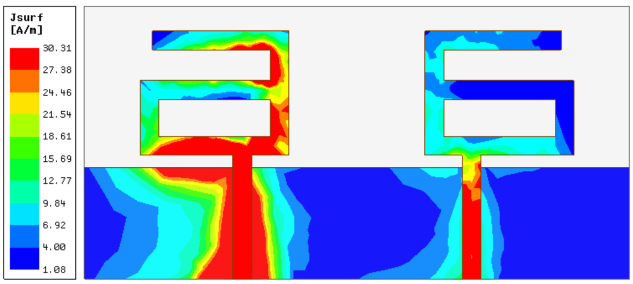

FIGURE 6. Current distribution of the corresponding two element antenna at 2.5 GHz.

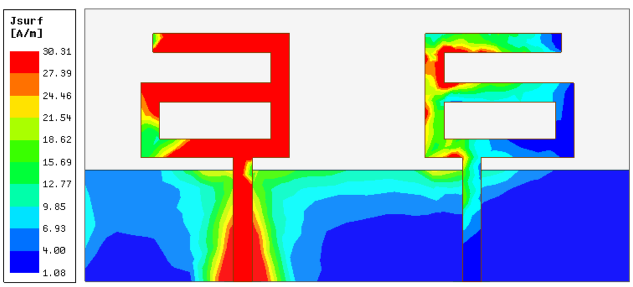

FIGURE 7. Current distribution of the corresponding two element antenna at 3.68 GHz.

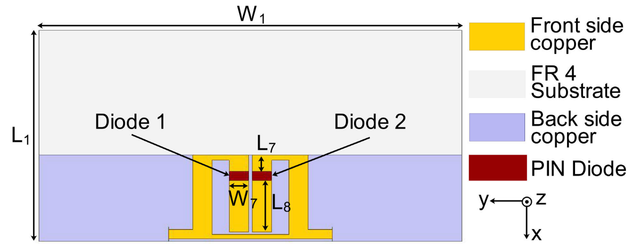

FIGURE 8. Diode integrated filter structure.

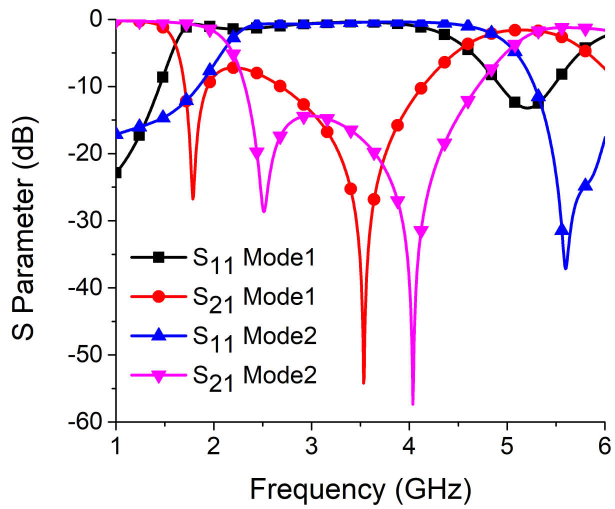

FIGURE 9. Bandstop filter characteristics under Mode 1 and Mode 2.

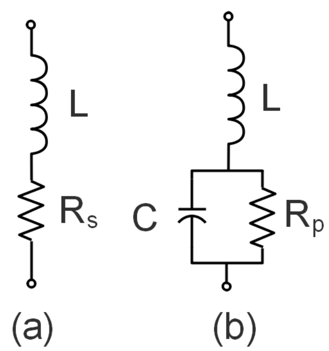

FIGURE 10. PIN diode equivalent circuit models (a) ON condition (b) OFF condition.

The OFF state of a PIN diode have shunt capacitance and reverse resistance of C = 0.23 pF and Rp = 0.4 MΩ, respectively. The series inductance value is 0.16 μH.

D. RECONFIGURABLE MIMO ANTENNA DEVELOPMENT

In the final phase, the reconfigurable bandstop filter designed in phase C is placed as a decoupling network between two antenna elements designed in phase B, as displayed in Fig 11. It is evident from the surface current distribution shown in Fig 12 and Fig 13, that the reconfigurable bandstop filter is able to reduce mutual coupling at 3.68 GHz and 2.5 GHz under Mode 1 and Mode 2 respectively with the inclusion of a decoupling network. However, the inclusion of a decoupling network causes impedance matching at 3.68 GHz to get deteriorated. So, in the final structure, two open circuit stub lines (W_9 = 2 mm) are introduced to achieve deep resonance at 3.68 GHz as shown in Fig 14. Thus a reconfigurable two port MIMO antenna has been developed using the reconfigurable bandstop filter isolation concept. The S-parameter characteristics under Mode 1 and Mode 2 conditions are shown in Fig 15.

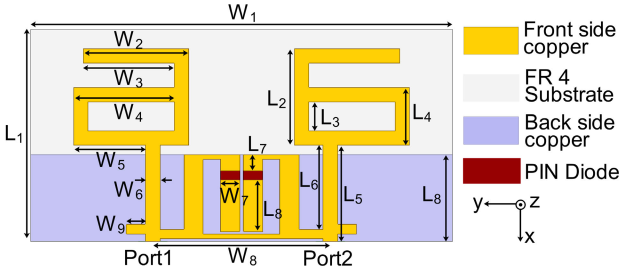

FIGURE 11. Complete antenna structure.

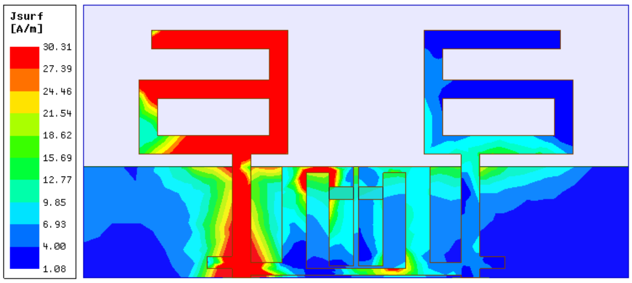

FIGURE 12. Surface current distribution of complete antenna at 3.68 GHz.

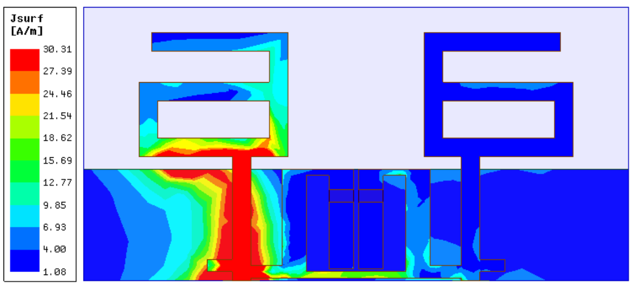

FIGURE 13. Surface current distribution of complete antenna at 2.5 GHz.

III. PARAMETRIC ANALYSIS

Simulation has been carried out to identify the parameters responsible for lower and upper band resonance on single antenna structure. It is found that L_5 causes the antenna to resonate at 2.5 GHz while W_2 is responsible for 3.68 GHz resonance. A parametric analysis has been conducted to display the variation of resonance for different lengths of L_5 and W_2 as shown in Fig 16 and Fig 17.

The spacing (W_8) between two antenna elements has a significant influence over isolation (S_{21}). As shown in Fig 18, the isolation increase with the increase of spacing between the two antenna elements. But the compact dimension of an antenna cannot be compromised for increasing the spacing. Therefore, a decoupling network is required to improve the isolation in the antenna without compromising the overall dimension.

An analysis is conducted to find the effect of the length of L_7 under Mode 2 (Both D1 and D2 OFF) on resonance at lower band. It is found that under switch off conditions

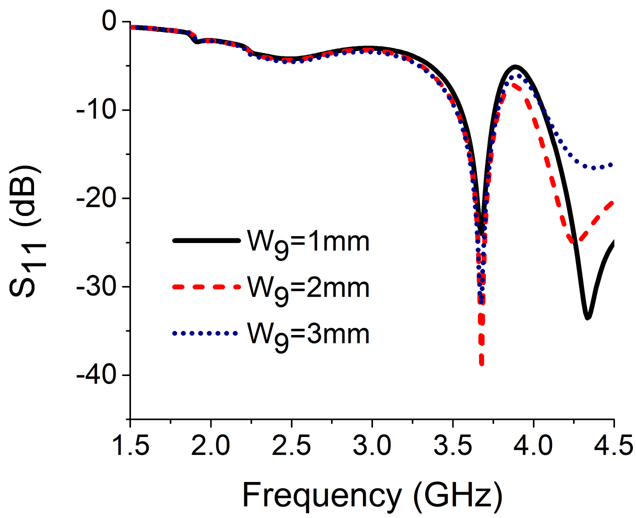

FIGURE 14. Effect of W_9 on resonance.

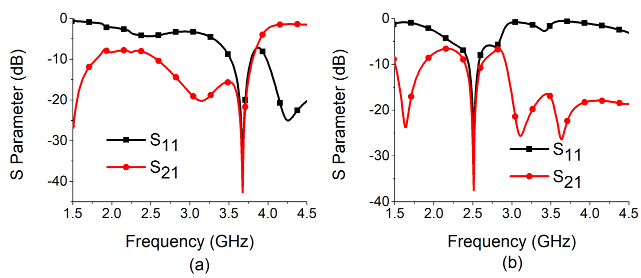

FIGURE 15. Simulated isolation and resonance at (a) 3.69 GHz (b) 2.5 GHz.

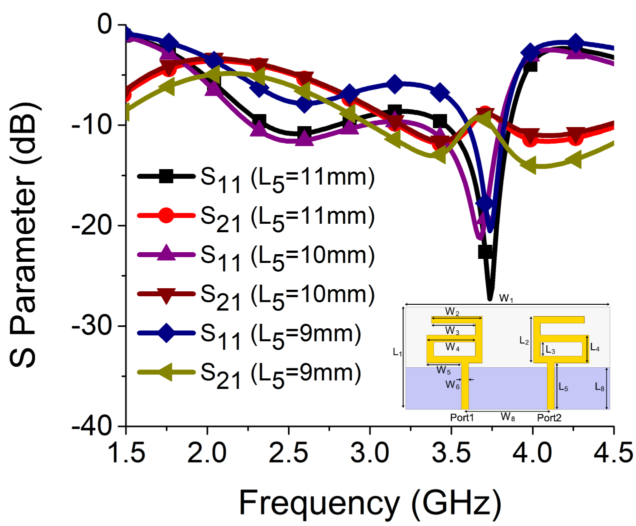

FIGURE 16. Effect of L_5 on lower band.

(Fig 19), the variation in the length of L_7 has negligible influence on resonance at 2.5 GHz.

But the position of switches in the bandstop filter has a significant influence on the resonance as shown in Fig 20. It is been observed that both resonance and isolation occurred

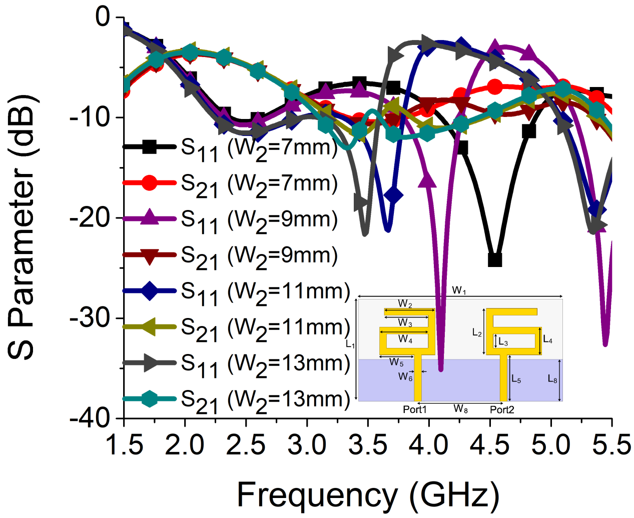

FIGURE 17. Effect of W_2 on upper band.

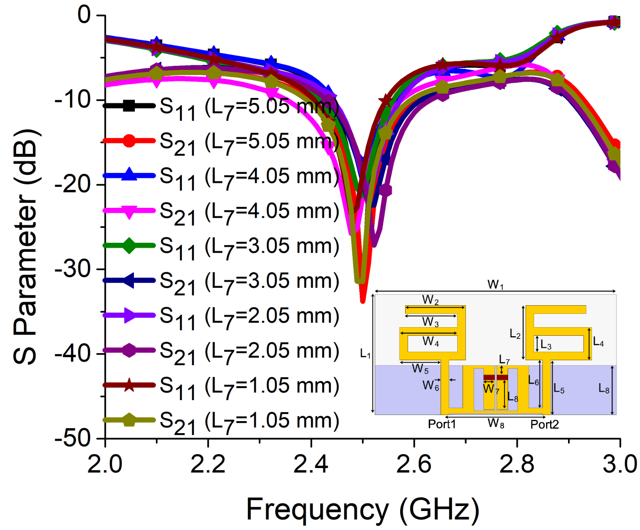

FIGURE 19. Effect of L_7 on resonance and isolation.

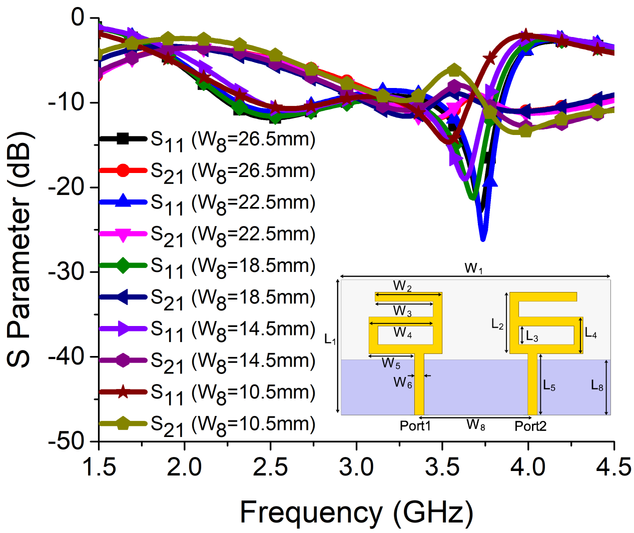

FIGURE 18. Effect of W_8 on resonance and isolation.

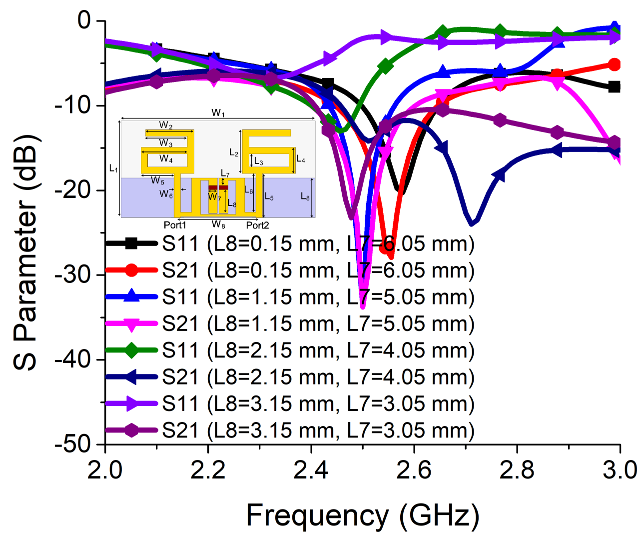

FIGURE 20. Effect of L_8 and L_7 on resonance and isolation.

at the same position only when $L_8 = 1.15$ mm and $L_7 = 5.05$ mm.

Fig 21 shows the improvement in resonance at 3.68 GHz with the increase in stub line length and optimal achieves at $W_9 = 2$ mm.

IV. RESULTS AND DISCUSSIONS

Fig 22 shows a prototype with a reconfiguration circuit required for verification of simulated results by measurement. Switching conditions and resonating frequencies under Mode 1 and Mode 2 are mentioned in Table 1. Three different classes of experiments conducted under both the switching options are: Scattering parameters measurement, Gain, Efficiency and Radiation pattern measurement, and Diversity parameters measurements. Results of three categories of experiments are detailed below.

TABLE 1. Switching mode combination.

Modes	D1	D2	Antenna frequency
Mode 1	ON	ON	3.68 GHz
Mode 2	OFF	OFF	2.50 GHz

A. SCATTERING PARAMETERS MEASUREMENT

Fig 23 verifies the simulation results with measured results for return loss and insertion loss of the MIMO antenna under Mode 1 and Mode 2 conditions. So, the upper (3.68 GHz) and lower (2.5 GHz) band MIMO operations can be controlled by the switching function of bandstop filter. The PIN diode integrated reconfigurable bandstop filter is able to bring high isolation for both the resonating frequencies of MIMO antenna. Maximum isolation of 42.77 dB

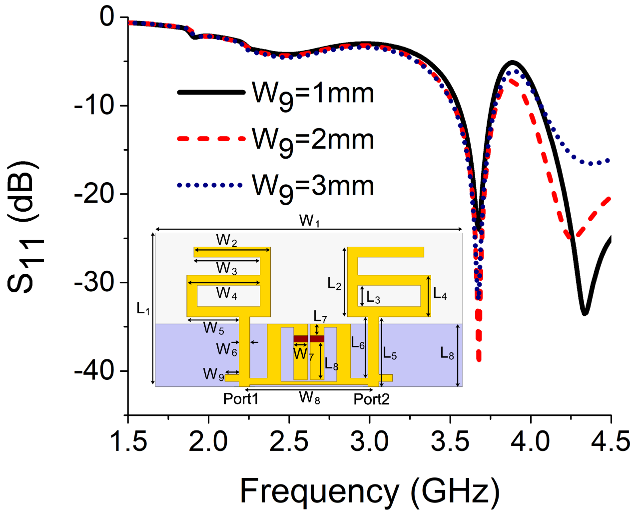

FIGURE 21. Effect of W_9 on resonance.

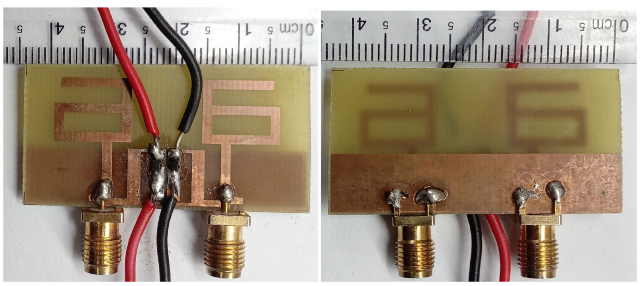
(a) (b)

FIGURE 22. Fabricated prototype model of proposed two-port MIMO antenna: (a) front view (b) back view.

and return loss of 39.41 dB is obtained at 3.68 GHz under Mode 1 while maximum isolation of 37.49 dB and reflection coefficient of 24.64 dB is obtained at 2.5 GHz under Mode 2. The operational bandwidth obtained at operating frequency 3.68 GHz and 2.5 GHz are 280 MHz (3.51 GHz–3.79 GHz) and 170 MHz (2.43 GHz–2.60 GHz) respectively. The disparity between simulation and measurement in some outband positions could be attributable to the presence of four DC lines in the prototype model and flaws in the fabrication process.

B. GAIN, EFFICIENCY AND RADIATION PATTERN MEASUREMENT

The peak gain and antenna efficiency are displayed in Fig 24 for both modes. It ensures the application of proposed antenna for successful transmission as well as the reception for radio communication. The proposed MIMO antenna exhibits peak gain of 2.97 dBi and 3.07 dBi and antenna efficiency of 86.8% and 91.47% at Mode 1 and Mode 2 respectively.

The presence of four DC lines in the prototype as shown in Fig 22, slightly degrades the gain and efficiency in the experimental environment for the proposed antenna.

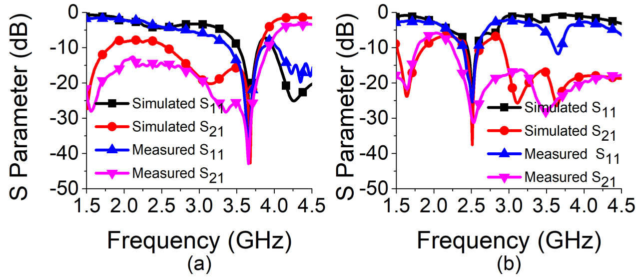

FIGURE 23. S_{11} and S_{21} measured and simulated for upper and lower band.

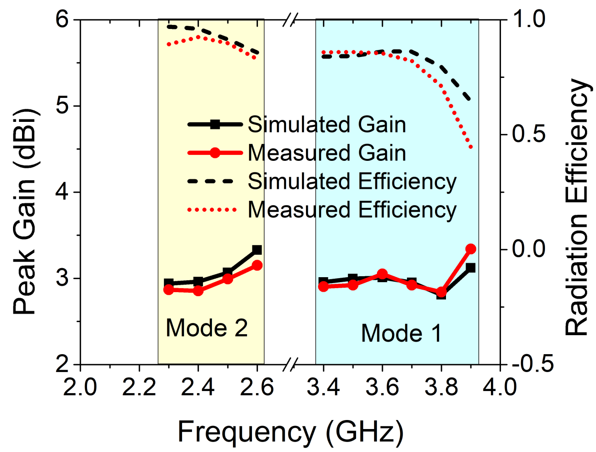

FIGURE 24. Peak gain and radiation efficiency of the proposed design.

Radiation pattern of the proposed antenna for both the modes is presented with E plane & H plane co and cross polarization shown in Fig 25 and Fig 26 respectively. It confirms good coverage of surrounding area by radiated power for both the frequency bands.

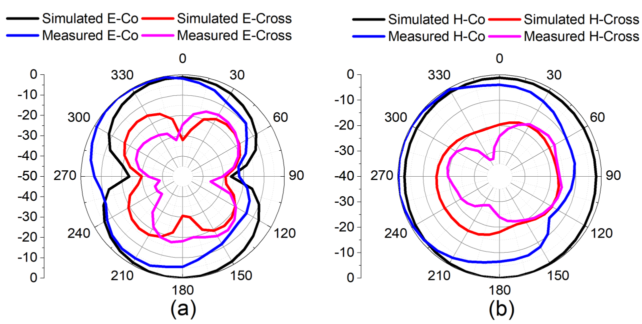

FIGURE 25. Normalized radiation pattern at 3.68 GHz (a) E Plane (b) H Plane.

C. DIVERSITY PARAMETERS MEASUREMENTS

In addition to the scattering matrix and radiation pattern, diversity performance metrics such as Envelope Correlation Coefficient (ECC), Diversity Gain (DG), Total Active Reflection Coefficient (TARC), Mean Effective Gain (MEG), and Channel Capacity Loss (CCL) should be measured to ensure

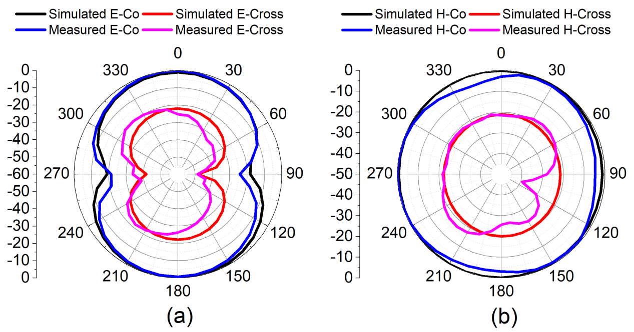

FIGURE 26. Normalized radiation pattern at 2.5 GHz (a) E Plane (b) H Plane.

that the MIMO antenna is making the efficient use of the surrounding environment. A sketch depicting the details of diversity metrics of the proposed MIMO antenna for both the upper and lower band is shown in Fig 27.

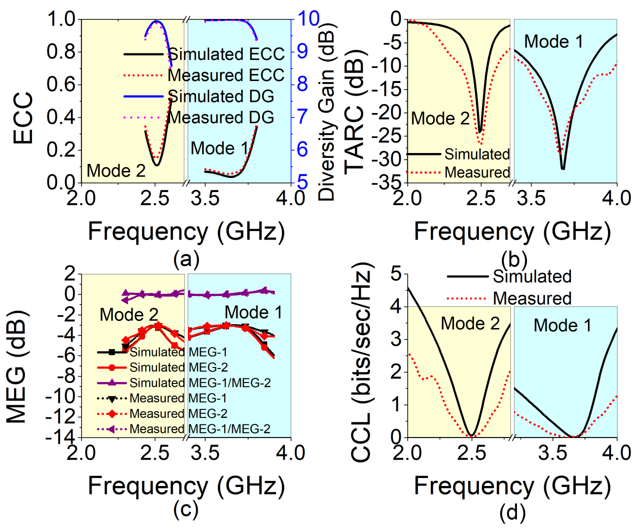

FIGURE 27. Simulated and measured results of proposed MIMO antenna, (a) ECC and diversity gain (DG), (b) TARC, (c) MEG, and (d) CCL.

ECC is a measure used to describe the isolation or correlation of communication channels, and it is defined in Eq. 1. Although the ideal value of ECC is 0, in practise, values less than 0.5 are acceptable. As shown in Fig 27a, it is evident that ECC is well below the acceptable limit for both the modes of proposed antenna at desired frequencies [27].

$$ECC = \frac{|\iint_{4\pi}\left[\overline{F_1}(\theta,\phi)\cdot\overline{F_2}(\theta,\phi)d\Omega\right]|^2}{\iint_{4\pi}|\overline{F_1}(\theta,\phi)|^2 d\Omega \iint_{4\pi}|\overline{F_2}(\theta,\phi)|^2 d\Omega} \tag{1}$$

In order to achieve good quality and reliability in wireless systems, the DG of the MIMO design should be high, reaching 10 dB in the operating bandwidth. Eq. 2 [28] is used to calculate the DG from the ECC value.

$$DG = 10 \times \sqrt{1-|ECC|} \tag{2}$$

TABLE 2. Simulated and measured results.

Antenna metrics	3.68 GHz (Mode 1)		2.50 GHz (Mode 2)	
	Simulated	Measured	Simulated	Measured
Isolation	-42.77dB	-40.77 dB	-37.49dB	-30.57 dB
Resonance	-39.41dB	-37.33 dB	-24.64dB	-25.35 dB
Bandwidth	280MHz	430 MHz	170MHz	220 MHz
Peak gain	2.97dBi	2.92 dBi	3.07dBi	2.98 dBi
Antenna Efficiency	86.8%	83.4%	91.47%	89.8%
ECC	0.049	0.067	0.115	0.154
DG	9.988	9.978	9.934	9.880
TARC	-32.02991	-26.02411	-24.14031	-26.72825
MEG1	-3.02009	-3.02152	-3.13958	-3.04488
MEG2	-3.04986	-3.14381	-3.07986	-3.0594
MEG1/MEG2	0.02977	0.12228	-0.05972	0.01452
CCL	0.01641	0.04812	0.06622	0.02853

Fig 27a depicts the DG of the proposed uniquely shaped switchable MIMO structure. It can be observed that the DG of the antenna in the desired bands for both modes is around 10 dB.

TARC is a real number between 0 and 1 that is defined as the square root of the ratio of the total available power to the sum of the power accessible at all ports minus the radiated power [29]. When the TARC value is zero, the available power is radiated completely. The total power available on all ports of the antenna system is the available power. TARC curves are used to determine the effective operating bandwidth of the antenna.

The general formula for determining TARC from the measured S-parameters for antennas with high efficiencies is given by

$$\Gamma_a^t = \frac{\sqrt{\sum_{i=1}^{N}|b_i|^2}}{\sqrt{\sum_{i=1}^{N}|a_i|^2}} \tag{3}$$

The expression of TARC, can also be evaluated by from the values of scattering matrix as mentioned in Eq. 4 [30].

$$\Gamma_a^t = \sqrt{\frac{((|S_{11}+S_{12}e^{j\theta}|^2)+(|S_{21}+S_{22}e^{j\theta}|^2))}{2}} \tag{4}$$

The evaluated TARC values for the proposed antenna for Mode 1 and Mode 2 are displayed in Fig 27b. The result ensures satisfactory MIMO operation at desired bands.

MEG calculates the gain of a MIMO antenna while taking into account the impacts of the surrounding environment. As shown in Fig 27c, the MEG analysis for the proposed antenna is performed at port 1 and port 2 for Mode 1 and Mode 2, respectively, using the formulas in Eq. 5 and Eq. 6 [31].

$$MEG_1 = 0.5[1-|S_{11}|^2-|S_{12}|^2] \tag{5}$$
$$MEG_1 = 0.5[1-|S_{12}|^2-|S_{22}|^2] \tag{6}$$

The MEG-1/MEG-2 ratio must be less than 3 dB for a successful MIMO antenna design with similar power levels.

TABLE 3. Comparative analysis of the proposed structure with some similar antennas.

Ref.	Dimension	No. of ports	Reconfiguration Technique	Isolation Technique	Frequency re-configurability options	Design Complexity	Max Isolation (dB)	Isolation Improve-ment (dB)	Gain (dBi)	ECC	DG (dB)	CCL (bits/s/ Hz)
[22]	$0.3\lambda_o \times 0.14\lambda_o$ (f=3 GHz)	2	PIN Diodes	Decoupling structure on the ground plane	I. 3-12 GHz II. 3.2-3.8 GHz	Moderate	>25	10	2.8 -1.1	<0.001	—-	<0.5 >0.5
[23]	$0.64\lambda_o \times 0.32\lambda_o$ (f=2.4 GHz)	2	PIN Diodes	An isolation improvement structure (IIS) is constructed on the ground plane	I. 2.4-2.483 GHz, 5.15-5.35 GHz II. 3.4-3.6 GHz	Complex	>20	—-	3.81, 1.87 5.15	<0.02, <0.002 <0.002	—-	—-
[33]	$0.71\lambda_o \times 0.39\lambda_o$ (f=2.35 GHz)	2	PIN Diodes	Band-notched quarter-wave slot line on the ground plane is used between the two recon-figurable antennas	I. 2.3-2.4 GHz II. 2.5-2.7 GHz III. 3.4-3.6 GHz	Complex	47 43 30.8	37.95 33.16 19.16	1.39 1.99 2.78	0.1108 0.0788 0.0056	9.35 9.37 9.61	10.29 10.61 11.45 (SNR of 20dB per port)
[34]	$0.6\lambda_o \times 0.3\lambda_o$ (f=1.5GHz)	2	Combination of PIN and Varac-tor diodes	Increasing spacing between antenna elements	I. 1-4.5 GHz II. 0.9-2.6 GHz	Moderate	>12.5	2.5	3.98 2.65	0.162 0.185	—-	—-
[24]	$0.012\lambda_o \times 0.3\lambda_o$ (f=0.72GHz)	2	PIN Diodes	Mounting the MIMO antenna on the vertical side edges of a laptop	I. 704-787 MHz II. 791-862 MHz, 2500-2690 MHz	Complex	>20	—-	—-	<0.0161	—-	—-
Prop. Work	$0.36\lambda_o \times 0.18\lambda_o$ (f=2.5GHz)	2	PIN Diodes	BSF decoupling n/w	I. 3.51-3.79 GHz II. 2.43-2.6 GHz	Simple	42.77 37.49	31.77 32.49	2.92 2.98	0.067 0.154	9.978 9.880	0.04812 0.02853

BSF: Bandstop Filter

The ratio for both modes of the planned MIMO antenna is significantly below 3 dB, as shown in Fig 27c.

The CCL calculates the maximum limit of channel loss at which message transmission can be carried out satisfactorily in a communication channel. The acceptable CCL must be limited to 0.4 bits/s/Hz for successful communication. The CCL using the S-parameters is calculated from Eq. 7-8 [32].

$$C_{loss} = -log_2|\varphi^R| \tag{7}$$

$$\varphi^R = \begin{bmatrix} \varphi_{11} & \varphi_{12} \\ \varphi_{21} & \varphi_{22} \end{bmatrix} \tag{8}$$

where

$$\begin{aligned}
\varphi_{11} &= 1 - (|S_{11}|^2 + |S_{12}|^2) \\
\varphi_{22} &= 1 - (|S_{22}|^2 + |S_{21}|^2) \\
\varphi_{12} &= -(S_{11}^* S_{12} + S_{21}^* S_{22}) \\
\varphi_{21} &= -(S_{22}^* S_{21} + S_{12}^* S_{11})
\end{aligned}$$

Fig. 27d shows the CCL calculated using S-parameters. For both Mode 1 and Mode 2, the CCL value is substantially lower than the maximum limit for the desired communication frequencies.

A comparison table of simulated and measured values of different antenna metrics for both the communication bands are listed in Table 2 for easy reference.

V. COMPARATIVE ANALYSIS

Table 3 includes a comparison of proposed reconfigurable MIMO antenna with few recently reported two port MIMO antennas. Mainly diode based reconfiguration has been considered for comparison. The isolation techniques that have been adapted in the papers are also mentioned in the table. It is found that proposed reconfigurable MIMO antenna is able to bring higher isolation at both the operating frequencies than the antennas reported in the table except [33]. The proposed bandstop filter decoupling technique also causes significant improvement in isolation for reconfigurable MIMO antenna. In addition to high isolation, it has a smaller dimension than the antennas listed in [23], [33], [34] and a larger dimension than the antennas mentioned in [22], [24]. The proposed antenna gain value is comparable to that of other work presented in the table. The proposed antenna has a higher ECC value than the work presented in [22]–[24], but most of the previous work [22], [23] measured ECC using the scattering parameter, whereas the proposed antenna measures ECC using the far-field radiation pattern. In comparison to other MIMO antennas the proposed MIMO antenna has a high directive gain, a vary low channel capacity loss, a moderate gain, and a simple structure. So, the proposed MIMO antenna has significant advantages over many previously reported antennas.

VI. CONCLUSION

In this work, a switchable bandstop filter is used as decoupling structure for developing miniaturised reconfigurable multiple input multiple output (MIMO) antenna. The switchable band stop filter is designed with unit cell split ring resonator and is deployed as a decoupling network between two closely spaced monopole antennas. Controlling the switching action of filter, the same MIMO antenna is operated at 3.68 GHz (Mode 1) and 2.5 GHz (Mode 2) with isolation 42.77 dB and 37.49 dB respectively. The proposed MIMO antenna exhibits peak gain of 2.97 dBi and 3.07 dBi and antenna efficiency of 86.8% and 91.47% at Mode 1 and Mode 2 respectively. For both the modes, diversity parameters like ECC, DG, TARC, MEG and CCL are observed along with key antenna performance metrics. Acceptable results are obtained for all parameters in the desired frequency bands. Simulation results are verified by measured results for the proposed antenna structure. The proposed isolation technique could also be used in future to design larger reconfigurable MIMO antennas with more than two antenna elements.

REFERENCES

[1] M. S. Sharawi, "Printed multi-band MIMO antenna systems and their performance metrics [wireless corner]," *IEEE Antennas Propag. Mag.*, vol. 55, no. 5, pp. 218–232, Oct. 2013.

[2] Y. J. Guo, P.-Y. Qin, S.-L. Chen, W. Lin, and R. W. Ziolkowski, "Advances in reconfigurable antenna systems facilitated by innovative technologies," *IEEE Access*, vol. 6, pp. 5780–5794, 2018.

[3] Z. Li, Z. Du, and K. Gong, "Compact reconfigurable antenna array for adaptive MIMO systems," *IEEE Antennas Wireless Propag. Lett.*, vol. 8, pp. 1317–1320, 2009.

[4] R. Hussain, M. S. Sharawi, and A. Shamim, "4-element concentric pentagonal slot-line-based ultra-wide tuning frequency reconfigurable MIMO antenna system," *IEEE Trans. Antennas Propag.*, vol. 66, no. 8, pp. 4282–4287, Aug. 2018.

[5] A. Mansoul, F. Ghanem, M. R. Hamid, and M. Trabelsi, "A selective frequency-reconfigurable antenna for cognitive radio applications," *IEEE Antennas Wireless Propag. Lett.*, vol. 13, pp. 515–518, 2014.

[6] I. Shah, S. Hayat, A. Basir, M. Zada, S. Shah, and S. Ullah, "Design and analysis of a hexa-band frequency reconfigurable antenna for wireless communication," *AEU-Int. J. Electron. Commun.*, vol. 98, pp. 80–88, Jan. 2019.

[7] K. Y. Chan, S. Fouladi, R. Ramer, and R. R. Mansour, "RF MEMS switchable interdigital bandpass filter," *IEEE Microw. Wireless Compon. Lett.*, vol. 22, no. 1, pp. 44–46, Jan. 2012.

[8] M. Sanchez-Renedo, R. Gomez-Garcia, J. Alonso, and C. Briso-Rodriguez, "Tunable combline filter with continuous control of center frequency and bandwidth," *IEEE Trans. Microw. Theory Techn.*, vol. 53, no. 1, pp. 191–199, Jan. 2005.

[9] C. Lugo and J. Papapolymerou, "Six-state reconfigurable filter structure for antenna based systems," *IEEE Trans. Antennas Propag.*, vol. 54, no. 2, pp. 479–483, Feb. 2006.

[10] M. S. Sharawi, A. B. Numan, and D. N. Aloi, "Isolation improvement in a dual-band dual-element MIMO antenna system using capacitively loaded loops," *Prog. Electromagn. Res.*, vol. 134, pp. 247–266, 2013.

[11] S. C. Chen, Y. S. Wang, and S. J. Chung, "A decoupling technique for increasing the port isolation between two strongly coupled antennas," *IEEE Trans. Antennas Propag.*, vol. 56, no. 12, pp. 3650–3658, Dec. 2008.

[12] H. Lee and B. Lee, "Compact broadband dual-polarized antenna for indoor MIMO wireless communication systems," *IEEE Trans. Antennas Propag.*, vol. 64, no. 2, pp. 766–770, Feb. 2016.

[13] C.-M. Luo, J.-S. Hong, and L.-L. Zhong, "Isolation enhancement of a very compact UWB-MIMO slot antenna with two defected ground structures," *IEEE Antennas Wireless Propag. Lett.*, vol. 14, pp. 1766–1769, 2015.

[14] R. Anitha, P. V. Vinesh, K. C. Prakash, P. Mohanan, and K. Vasudevan, "A compact quad element slotted ground wideband antenna for MIMO applications," *IEEE Trans. Antennas Propag.*, vol. 64, no. 10, pp. 4550–4553, Oct. 2016.

[15] S.-W. Su, C.-T. Lee, and F.-S. Chang, "Printed MIMO-antenna system using neutralization-line technique for wireless USB-dongle applications," *IEEE Trans. Antennas Propag.*, vol. 60, no. 2, pp. 456–463, Feb. 2012.

[16] M. M. Bait-Suwailam, M. S. Boybay, and O. M. Ramahi, "Electromagnetic coupling reduction in high-profile monopole antennas using single-negative magnetic metamaterials for MIMO applications," *IEEE Trans. Antennas Propag.*, vol. 58, no. 9, pp. 2894–2902, Sep. 2010.

[17] A. A. Althuwayb, "Low-interacted multiple antenna systems based on metasurface-inspired isolation approach for MIMO applications," *Arabian J. Sci. Eng.*, pp. 1–10, May 2021, doi: 10.1007/s13369-021-05720-6.

[18] M. Alibakhshikenari, F. Babaeian, B. S. Virdee, S. Aïssa, L. Azpilicueta, C. H. See, A. A. Althuwayb, I. Huynen, R. A. Abd-Alhameed, F. Falcone, and E. Limiti, "A comprehensive survey on 'various decoupling mechanisms with focus on metamaterial and metasurface principles applicable to SAR and MIMO antenna systems,'" *IEEE Access*, vol. 8, pp. 192965–193004, 2020.

[19] M. Alibakhshikenari, B. S. Virdee, N. O. Parchin, P. Shukla, K. Quazzane, C. H. See, R. Abd-Alhameed, F. Falcone, and E. Limiti, "Isolation enhancement of densely packed array antennas with periodic MTM-photonic bandgap for SAR and MIMO systems," *IET Microw., Antennas Propag.*, vol. 14, no. 3, pp. 183–188, Mar. 2019.

[20] M. Alibakhshikenari, M. Khalily, B. S. Virdee, C. H. See, R. A. Abd-Alhameed, and E. Limiti, "Mutual-coupling isolation using embedded metamaterial EM bandgap decoupling slab for densely packed array antennas," *IEEE Access*, vol. 7, pp. 51827–51840, 2019.

[21] M. Alibakhshikenari, M. Khalily, B. S. Virdee, C. H. See, R. Abd-Alhameed, and E. Limiti, "Mutual coupling suppression between two closely placed microstrip patches using EM-bandgap metamaterial fractal loading," *IEEE Access*, vol. 7, pp. 23606–23614, 2019.

[22] A. Quddus, R. Saleem, and M. F. Shafique, "Compact electronically reconfigurable WiMAX band-notched ultra-wideband MIMO antenna," *Radioengineering*, vol. 27, no. 4, pp. 1–8, 2018.

[23] Z.-J. Jin, J.-H. Lim, and T.-Y. Yun, "Frequency reconfigurable multiple-input multiple-output antenna with high isolation," *IET Microw., Antennas Propag.*, vol. 6, no. 10, pp. 1095–1101, Jul. 2012.

[24] B. Mun, C. Jung, M.-J. Park, and B. Lee, "A compact frequency-reconfigurable multiband LTE MIMO antenna for laptop applications," *IEEE Antennas Wireless Propag. Lett.*, vol. 13, pp. 1389–1392, 2014.

[25] S. R. Thummaluru and R. K. Chaudhary, "Mu-negative metamaterial filter-based isolation technique for MIMO antennas," *Electron. Lett.*, vol. 53, no. 10, pp. 644–646, 2017.

[26] P. Garg and P. Jain, "Isolation improvement of MIMO antenna using a novel flower shaped metamaterial absorber at 5.5 GHz WiMAX band," *IEEE Trans. Circuits Syst. II, Exp. Briefs*, vol. 67, no. 4, pp. 675–679, Apr. 2020.

[27] S. Blanch, J. Romeu, and I. Corbella, "Exact representation of antenna system diversity performance from input parameter description," *Electron. Lett.*, vol. 39, no. 9, pp. 705–707, May 2003.

[28] A. W. M. Saadh, K. Ashwath, P. Ramaswamy, T. Ali, and J. Anguera, "A uniquely shaped MIMO antenna on FR4 material to enhance isolation and bandwidth for wireless applications," *AEU-Int. J. Electron. Commun.*, vol. 123, Aug. 2020, Art. no. 153316.

[29] M. S. Sharawi, "Printed MIMO antenna systems: Performance metrics, implementations and challenges," *Forum Electromagn. Res. Methods Appl. Technol.*, vol. 1, pp. 1–11, Feb. 2014.

[30] T. Kumari, G. Das, A. Sharma, and R. K. Gangwar, "Design approach for dual element hybrid MIMO antenna arrangement for wideband applications," *Int. J. RF Microw. Comput.-Aided Eng.*, vol. 29, no. 1, Jan. 2019, Art. no. e21486.

[31] G. Das, A. Sharma, and R. K. Gangwar, "Dielectric resonator based circularly polarized MIMO antenna with polarization diversity," *Microw. Opt. Technol. Lett.*, vol. 60, no. 3, pp. 685–693, Mar. 2018.
[32] G. A. Sarkar, S. Ballav, A. Chatterjee, S. Ranjit, and S. K. Parui, "Four element MIMO DRA with high isolation for WLAN applications," *Prog. Electromagn. Res. Lett.*, vol. 84, pp. 99–106, 2019.
[33] J.-H. Lim, Z.-J. Jin, C.-W. Song, and T.-Y. Yun, "Simultaneous frequency and isolation reconfigurable MIMO PIFA using PIN diodes," *IEEE Trans. Antennas Propag.*, vol. 60, no. 13, pp. 5939–5946, Dec. 2012.
[34] X. Zhao, S. Riaz, and S. Geng, "A reconfigurable MIMO/UWB MIMO antenna for cognitive radio applications," *IEEE Access*, vol. 7, pp. 46739–46747, 2019.

HASHINUR ISLAM (Graduate Student Member, IEEE) received the B.Tech. degree in electronics and telecommunication engineering from the Institute of Electronics and Telecommunication Engineers (IETE), India, in 2014, and the M.Tech. degree in digital electronics and communication engineering from the Sikkim Manipal Institute of Technology, Sikkim Manipal University, in 2018, where he is currently pursuing the Ph.D. degree.

He has published over 16 refereed articles in journals and conference proceedings. His research interests include multiband antennas, fractal antenna, circular polarization on antennas, feeding mechanism for antenna, PIFA antenna, wearable antenna, antenna for embedded systems, microstrip filters, and MIMO antenna. He is an Associate Member of IETE India. He is a Reviewer of IEEE ACCESS and the *International Journal of Microwave and Wireless Technologies* (Cambridge University Press).

SAUMYA DAS received the B.Tech. degree in electronics and telecommunication engineering from the Institute of Electronics and Telecommunication Engineers (IETE), India, the M.E. degree in electronics and communication engineering from the Delhi College of Engineering, University of Delhi, and the Doctor of Philosophy degree in electronics and communication engineering from Sikkim Manipal University.

He is currently an Assistant Professor with the Department of Information Technology, Sikkim Manipal Institute of Technology, India. He has more than 15 years of teaching experience with expertise in various subjects, such as electromagnetic field theory, antenna theory, microwave devices and circuits, signals and systems, digital signal processing, and adaptive signal processing. He has published several articles in reputed peer-reviewed international journals and conferences. His research interests include different feeding techniques for microstrip and dielectric resonator antennas, flexible and wearable antenna for tracking and medical application, computational mathematics for antenna designing, RF exposure testing on human-bodies, electromagnetic compatibility, and ultra wideband antenna designing. He is an Associate Member of IETE, India. He serves as a Reviewer for *Microwave and Optical Technology Letters*—MOTL (Wiley) and *IETE Journal of Research* (Taylor & Francis).

TANWEER ALI (Senior Member, IEEE) is currently an Assistant Professor-Senior Scale with the Department of Electronics and Communication Engineering, Manipal Institute of Technology, Manipal Academy of Higher Education, Manipal. He is also an Active Researcher in microstrip antennas, wireless communication, and microwave imaging. He has published more than 90 papers in reputed peer-reviewed international journals and conferences. He is a member of the IEEE Antenna and Propagation Society and an Associate Member of IETE, India. He serves on the board of reviewers for journals, such as the IEEE TRANSACTIONS ON ANTENNAS AND PROPAGATION, the IEEE ANTENNAS AND WIRELESS PROPAGATION LETTERS, IEEE ACCESS, the IEEE TRANSACTIONS ON MICROWAVE THEORY AND TECHNIQUES, the IEEE SENSORS JOURNAL, *IET Microwaves, Antennas and Propagation*, *Electronics Letters* (IET), *Wireless Personal Communications*—WPC (Springer), *AEU-International Journal of Electronics and Communications*, *Microwave and Optical Technology Letters*—MOTL (Wiley), the *International Journal of Antennas and Propagation* (Hindawi), *Advanced Electromagnetics*, *Progress in Electromagnetic Research* (PIER), *KSII Transactions on Engineering Science*, South Korea, the *International Journal of Microwave and Wireless Technologies*, *Frequenz*, and *Radioengineering*.

TANUSHREE BOSE received the Ph.D. degree in design of printed antennas using neural network from the Department of Electronics and Communication Engineering, BIT, Mesra, India, in 2011.

She worked in RF and microwave antennas with soft computation. She is currently an Associate Professor with the Sikkim Manipal Institute of Technology, India. She has published over 30 refereed articles in journals and conference proceedings. She has completed one Government (AICTE) Sponsored Research Project on Patch Antenna Designing Using Artificial Neural Network and successfully guided her research scholars. Her current research interests include multiband antennas for handsets and networks, miniature antennas, reconfigurable antennas, EBG application on conformal antennas, flexible and wearable antennas, and smart antennas. She has served on many national and international technical committees.

SUMANA KUMARI was born in India, in February 1979. She received the bachelor's and Master of Science degrees in electronics and telecommunication and the Ph.D. degree from the Birla Institute of Technology, Mesra, Ranchi, India, in September 2000, 2002, and 2012, respectively. She has been working as an Assistant Professor at University Polytechnic, BIT, since January 2003. Her research interests include printed antennas for wireless and mobile communications.

OM PRAKASH received the B.Tech. degree in electronics and telecommunication engineering from the Institute of Electronics and Telecommunication Engineers (IETE), India, the M.Tech. degree in instrumentation and control engineering from the Sant Longowal Institute of Engineering and Technology, Longowal, Punjab, India, and the Ph.D. degree in electronics and communication engineering from Shri Jagdish Prasad Jhabarmal Tibrewala University, Rajasthan, India. He is currently working with the Sri Venkateswara College of Engineering and Technology (Autonomous), Andhra Pradesh, India, as an Associate Professor with the Electronics and Communication Department. He has more ten years of teaching and research experience. He has one Indian patent and one book chapter. He is the author of more than 60 journals and conference papers. His research interests include power system optimization, image signal processing, antenna design, embedded systems, and wireless communication. He is a member of the Scientific and Industrial Research Organization, IETE, Delhi; and the International Association of Engineers (IAENG), Hong Kong.

PRADEEP KUMAR received the bachelor's, Master of Engineering, and Doctor of Philosophy degrees in electronics and communication engineering, in 2003, 2005, and 2009, respectively. He completed his postdoctoral studies from the Autonomous University of Madrid, Spain. He is currently working with the University of KwaZulu-Natal, South Africa. He has over 15 years of experience in academic and research. He has held various positions, such as a Lecturer, a Senior Lecturer, an Assistant Professor, and an Associate Professor. He is the author of many research papers published in various peer-reviewed journals/conferences. His current research interests include antennas, antenna arrays, and wireless communications. He is registered as a Professional Engineer with Engineering Council of South Africa. He received various awards/fellowships, such as a MHRD Fellowship, an A4U Fellowship, the Research Excellence Award, the J. W. Nelson Fund Research Award, and the CAES Research Award. He is serving as a Reviewer/TPC Member for many journals/conferences, such as IEEE TRANSACTIONS ON ANTENNAS AND PROPAGATION, IEEE ACCESS, *Progress in Electromagnetics Research*, *ACES Journal*, *IEEE Systems Journal*, *SAIEE Africa Research Journal*, the *International Journal of Electronics*, SATNAC, and IEEE Africon.